Inversion of neutron/gamma spectra from scintillator measurements

J. Köhler [a,*], B. Ehresmann [a], C. Martin [a], E. Böhm [a], A. Kharytonov [a], O. Kortmann [a,c], C. Zeitlin [b], D.M. Hassler [b], R.F. Wimmer-Schweingruber [a]

[a] IEAP, Christian Albrechts University, Kiel, Germany
[b] Southwest Research Institute, Department of Space Studies, Boulder, CO, United States
[c] Space Sciences Laboratory, Berkley, CA, United States

ABSTRACT

The Radiation Assessment Detector (RAD) on-board NASA's Mars Science Laboratory (MSL) rover will measure charged particles as well as neutron and gamma radiation on the Martian surface. Neutral particles are an important contribution to this radiation environment. RAD measures them with a CsI (Tl) and a plastic scintillator, which are both surrounded by an anticoincidence. The incident neutron/gamma spectrum is obtained from the measurements using inversion methods which often fit a functional behavior, e.g., a power law, to the measured data applying the instrument response function and, e.g., a least-squares method. In situations where count rates are small, i.e., where the stochastic nature of the measurement is evident, maximum likelihood estimates with underlying Poissonian statistics improve the resulting spectra. We demonstrate the measurement and inversion of gamma/neutron spectra for a detector concept featuring one high-density scintillator and one high-proton-content scintillator. The applied inversion methods derive the original spectra without any strong assumptions of the functional behavior. Instrument response functions are obtained from Monte-Carlo simulations in matrix form with which the instrument response is treated as a set of linear equations. Using the response matrices we compare a constrained least-squares minimization, a chi-squared minimization and a maximum likelihood method with underlying Poissonian statistics. We make no assumptions about the incident particle spectrum and the methods intrinsically satisfy the constraint of non-negative counts. We analyzed neutron beam measurements made at the Physikalisch Technische Bundesanstalt (PTB) and inverted the measurement data for both neutron and gamma spectra. Monte-Carlo-generated measurements of the expected Martian neutron/gamma spectra were inverted as well, here the maximum likelihood method with underlying Poissonian statistics produces significantly better results.

© 2011 Elsevier B.V. All rights reserved.

1. Introduction

Realizing neutron and gamma measurements on-board a spacecraft is often difficult due to the limitations of the instruments size and weight. One possible approach is the use of a combination of a high-proton-content and a high-density scintillator material which have different sensitivities for neutrons and gammas. This concept is used in the Radiation Assessment Detector (RAD) which is a part of the Mars Science Laboratory (MSL) mission and will measure the charged particle spectrum up to several 100 MeV/nuc and the neutron/gamma particle spectra up to 100 MeV on the surface of Mars. Unlike for stopping charged particles, where the energy deposit equals the particle energy, neutral particles create an energy deposit which can be randomly distributed and ranging up to their incident energy. Therefore, a measured spectrum does not necessarily reflect the energy spectrum of the incoming particles. However, using the measurement and a carefully modeled and calibrated instrument response function, the incoming particle spectrum can be determined by inversion methods.

The choice of inversion method is important to ensure its success. In our case in which we want to measure sometimes low count rates of neutral particles, this aspect is crucial. Because the number of counts may be very low or possibly even zero, the signals must be modeled as a Poissonian process, i.e., using Poissonian statistics. The correct statistical approach is the dominant factor for the investigation of such problems [1–4]. When the uncertainties or noise in the experimental data are distributed with Gaussian statistics the least-squares methods or other variants of chi-square minimization [5–7] can be used for the solution of inverse problems. One can easily show that the least-squares method is a maximum likelihood estimator of the fitted parameters if the measurements errors are independent and normally (Gaussian) distributed.

* Corresponding author. Tel.: +49 431 880 3944; fax: +49 431 880 3968.
 E-mail address: koehler@physik.uni-kiel.de (J. Köhler).

For an uncertainty distribution with Poisson statistics least-squares methods or minimizing chi-square do not maximize the likelihood that the fitted parameters reflect the data. The strategy of solving inverse problems with Poissonian noise is similar to the strategy of solving problems with Gaussian statistics but leads to more difficult optimization problems that are non-quadratic with non-negatively constrained and, possibly, with non-convex objective functions.

Using a log-likelihood function with Poissonian or Gaussian noise for a maximum likelihood solution one can formulate a variational problem that connects the known measurements with the unknown, but non-negative, original energy spectrum using the modeled and calibrated instrument response function.

The problem of obtaining model parameters from data which are distributed according to Poissonian statistics occurs in many practical applications such as medical imaging, remote sensing, optical microscopy, and astronomy. Therefore various maximum likelihood methods are used with different modifications that can accelerate the convergence of these algorithms [8] and increase the smoothness of the inverted data [9] or are used for wavelet, multiscale analysis or regularization methods [10,11].

In this paper we estimate the original energy spectrum of neutrons and gammas by inverting neutron and gamma scintillator measurements. We solve the non-linear inversion problem by optimization methods using Gaussian or Poissonian statistics. Similar inversion approaches, applied to counting experiments, have been considered in [12] and in [13].

The paper is organized as follows. In Section 1 we give a description of the RAD instrument and of the inversion methods used. In Section 2 we show the instrument response function, Section 3 describes the strategies for obtaining initial guesses and compares several inversion methods using well-defined neutron beam measurements. In Section 4 we apply and compare different inversion methods to Monte-Carlo generated measurements of the expected neutron/gamma fluxes at Martian surface and show that correct use of the Poissonian method yields the best results.

2. Methods

2.1. Instrumental background

The Radiation Assessment Detector (RAD) measures gammas and neutrons with two scintillators which are enclosed by an anticoincidence (see Fig. 1). One of the scintillators has a high sensitivity for gammas, the other has high sensitivity for neutrons. The surrounding anticoincidence prevents the measurement from being polluted by charged particles.

In this work, the inversion of the neutron/gamma spectra is performed for the RAD sensorhead which, in addition to gammas and neutrons, also measures charged particles. It is shown schematically in Fig. 1 and consists of several detectors. Charged particles are measured by a telescope of silicon detectors **A**, **B**, **C**, followed by to scintillators **D** and **E**. Besides the detection of charged particles the **D** and **E** scintillator are also used to detect neutral particles. The **D** scintillator, which consists of cesium iodide, is highly sensitive to gamma particles. The **E** detector, which consists of plastic, is highly sensitive to neutrons. For the detection of neutral particles the **C**, **F1/2** detectors are used as an anticoincidence. The energy analysis is done via pulse height analysis on-board, the measured spectra are sent back to earth.

Although the **D** scintillator in mainly sensitive to gamma radiation, it also detects a significant fraction of incident neutrons, similarly, the **E** detector also measures gammas. This ambiguity in the detector measurements leads to the need for four detector respo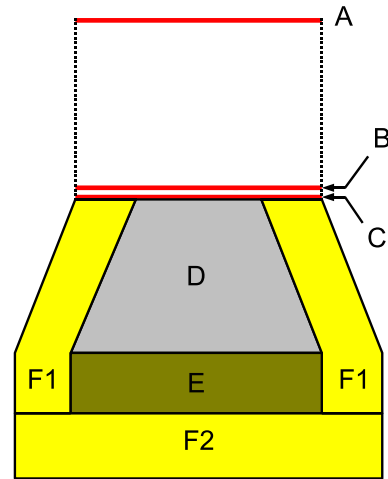nse matrices which need to be considered when inverting a measurement. In other words, we need one response function for **D** for gammas, one for **D** for neutrons, one for **E** for gammas, and one for **E** for neutrons.

Fig. 1. Schematic view of the RAD sensor head consisting of three silicon solid state detectors **A**, **B**, **C** (red), a CsI scintillator **D** (gray) and a the plastic scintillator **E** (dark yellow). Both scintillators are surrounded by a plastic anticoincidence **F1/2** (yellow). **A**, **B**, **C**, **D**, **E** are used as a telescope for charged particles. Neutral particles are detected in the **D**, and **E** scintillator in anticoincidence with **F1/2** and **C**.

In contrast to stopping particles in silicon, neutral particles do not create an energy deposit strictly proportional to the incident particles energy. For example, the electron cascade, caused by a high energy gamma, is not necessarily contained in the scintillator. Incident neutrons create secondary protons whose energies depend on the collision angle and are randomly distributed up to the energy of the incident neutron. Some protons can also escape from the scintillator before fully depositing their energy. Therefore, the detector response matrices are expected to show a roughly triangular shape and to be far from diagonal, as the response matrix for a perfect detector would be.

2.2. Mathematical background

Let us consider a spectrum of incoming neutron or gamma particles $\vec{f} = (f_1, f_2, \ldots, f_n)$, which is binned in the energy bins $\vec{E} = (E_1, \ldots, E_n)$. A mapping between a spectrum of incoming particles and the measured detector response $\vec{z} = (z_1, z_2, \ldots, z_n)$ can be performed by

$$\vec{z} = \mathbf{A} \cdot \vec{f}, \tag{1}$$

where the matrix $\mathbf{A}$ is the detector response matrix and the components of $\vec{z}$ are the counts per measurement bin, henceforth called measurements. One possible solution would be to fit a small number of parameters which describe a model for **f** to the large number of measurements **z**. Here, we will not follow this more traditional approach, but will attempt to perform a full inversion of the system (Eq. (1)). In other words, we optimize for the same number of parameters as there are measurements.

As described in the previous section, the **D** detector is also somewhat sensitive to neutrons while the **E** detector is somewhat sensitive to gammas. Unfortunately, it is not possible to distinguish between a neutron and a gamma signal in either detector. All we have available are the measurements in the **D** and **E** detectors, $\vec{z}_D$ and $\vec{z}_E$. These are the instrument responses to an input spectrum of neutrons $\vec{f}_N$ and gammas $\vec{f}_\gamma$. This can be described by

$$\vec{z_D} = \mathbf{A}_{D,\gamma} \cdot \vec{f_\gamma} + \mathbf{A}_{D,N} \cdot \vec{f_N} \tag{2}$$

$$\vec{z_E} = \mathbf{A}_{E,\gamma} \cdot \vec{f_\gamma} + \mathbf{A}_{E,N} \cdot \vec{f_N}. \tag{3}$$

Let us define the stacked vector $\vec{f} := \vec{f_\gamma} \oplus \vec{f_N} = (f_{1\gamma}, \ldots, f_{n\gamma}, f_{1N}, \ldots, f_{nN})$ and $\vec{z} = \vec{z_D} \oplus \vec{z_E}$. We can than apply Eq. (1), where $\mathbf{A}$ consists of the matrices of the $\mathbf{D}$ and $\mathbf{E}$ detector and each for neutrons and gammas

$$\mathbf{A} = \begin{pmatrix} \mathbf{A}_{D,\gamma} & \mathbf{A}_{D,N} \\ \mathbf{A}_{E,\gamma} & \mathbf{A}_{E,N} \end{pmatrix}.$$

In principle, we can now solve Eq. (1). However, this generally leads to non-physical results (such as negative counts) for three reasons. First, $\mathbf{A}$ is often singular and therefore the inverse matrix $\mathbf{A}^{-1}$ can not be obtained, nevertheless there exist several methods to obtain pseudo inverse matrices, e.g., the singular value decomposition, which can provide solutions of Eq. (1) [7]. Second, $\mathbf{A}$ is only known with limited accuracy which means that the exact Eq. (1) is not known. Third, the measurement vector contains measurement errors such as electronic noise, incomplete light collection, and statistical fluctuations. The latter means that a simple inversion of Eq. (1) ($\vec{f} = \mathbf{A}^{-1} \cdot \vec{z}$) does not consider the stochastic nature of the measurement process. For instance, a single incident particle is detected in one measurement channel only, it is not distributed over a wide range of channels which Eq. (1) would suggest.

These effects often lead to unphysical results such as negative values in $\vec{f}$. To obtain a non-negative solution of $\vec{f}$, the problem Eq. (1) can for instance be replaced by a constrained minimization problem, which can be formulated as a non-negative least-squares (NNLS) problem,

$$\min \sum_i \left(\sum_j a_{ij} f_j - z_i \right)^2, \quad \text{with } f_i \geqslant 0, \tag{4}$$

where a_{ij} are the components of the matrix $\mathbf{A}$. NNLS methods have been considered in [6,5]. As is true with other methods, the least-squares problem always has a solution but it is non-unique if the rank of the matrix $\mathbf{A}$ is less than its dimension n.

A similar method is given by the minimum chi-square method with constraints [7]:

$$\min \sum_i \left(\frac{\sum_j a_{ij} f_j - z_i}{\sigma_i^2} \right)^2, \quad \text{with } f_i \geqslant 0. \tag{5}$$

With $\sigma^2 = z_i$ one can consider Eq. (5) as a new variant of the minimum chi-square method [14].

Another way to solve the problem lies in reformulating it as a similar maximum likelihood problem with underlying Poisson statistics [12,13]. According to the Poisson distribution, the probability that a measurement with an expectation value of $\lambda_i = (\mathbf{A} \cdot \vec{f})_i$ results in z_i counts is given by

$$p(z_i, \lambda_i) = \frac{\lambda_i^{z_i} e^{-\lambda_i}}{z_i!}. \tag{6}$$

The corresponding probability function, $P(\vec{z}, \vec{f})$ that includes all parameters f_i and all independent measurements z_i, which maximizes the likelihood function $L(\vec{f})$, is given by

$$L(\vec{f}) = P(\vec{z}, \vec{f}) = \prod_{i=1}^n p(z_i, \lambda_i). \tag{7}$$

The corresponding log-likelihood function has the following form [3]

$$-l(\vec{f}) = \sum_i (\lambda_i - z_i \ln \lambda_i) + c, \tag{8}$$

where $c = \sum_i \ln(z_i!)$. For the estimation of the spectrum $\vec{f}$ we must solve the constrained minimization problem

$$\min \sum_i (\lambda_i - z_i \ln \lambda_i), \text{ with } f_i \geqslant 0. \tag{9}$$

We solve the optimization problems Eqs. (4), (5) and (9) with the constraints $f_i > 0 \; \forall f_i$ using the SciPy [15] implementation of the L-BFGS-B algorithm [16,17].

3. Monte-Carlo simulations of instrument response functions

In this section we explain the instrument response matrix for gammas and neutrons (i.e., of the $\mathbf{D}$ and $\mathbf{E}$ detectors). It shows our best effort at reproducing the behavior of the sensorhead in combination with the associated electronics.

The detector response matrix is calculated as described in [7], the energy deposits in the scintillators are calculated with GEANT4 [18]. To calculate the light output of the scintillator, which is measured by photodiodes, a ray-tracing Monte-Carlo-readout model is used [19]. Further, electronic noise is added and the light output is mapped to measurement channels as obtained from various calibration runs. Effects such as direct particle hits in the photodiodes are considered as well. We focus on energies ⩽19 MeV, where GEANT4 calculates neutron interaction with a model based on measurements. Above 20 MeV GEANT4 uses theoretical models which produces a discontinuity in the detector response, which we do not believe.

The resulting detector response matrix $\mathbf{A}$ is shown in Fig. 2. The range of the measurement bins was chosen to cover the whole range of relevant detector responses, the first bin (number 2500) is not influenced by the noise peak or the trigger threshold, compare Figs. 2 and 3.

4. Applying inversion methods to neutron beam measurements

In this section we compare measurements with simulations of the instrument response, and then proceed to invert the measurements using $\mathbf{A}$ as described in Section 2. For the inversion we use the L-BFGS-B algorithm which searches for the minimum of the given merit function, starting from an initial guess. To find a minimum close to the global minimum, several initial guesses are calculated which are used as a starting point for the L-BFGS-B algorithm.

4.1. Comparing measurement and simulation

As a test of the inversion methods we choose calibration measurements performed at the Physikalisch-Technische Bundesanstalt (PTB) in Braunschweig. The sensorhead was calibrated with 14.8 and 19 MeV neutron beams [20]. Before applying inversion methods the ability of the GEANT4 Monte Carlo and the photodiode readout model to predict the behavior of the sensorhead is tested.

Fig. 3 compares the calibration runs with GEANT4 simulations of monoenergetic 14.8 and 19 MeV neutron beams which enter the instrument (from above in Fig. 1). Measurements and simulation agree very well for both $\mathbf{D}$ and $\mathbf{E}$ detector. Because the trigger threshold is not included in the simulation we do not expect agreement in measurement channels ⩽2500. We can therefore assume, that the detector response matrix is able to describe both the 14.8 and 19 MeV run correctly.

4.2. The inversion: initial guesses and procedure

To obtain the measurement vector $\vec{z}$, the PTB measurements shown in Fig. 3 were rebinned to match the detector response matrix (Fig. 2). Since both the gamma and the neutron spectra now consist of 18 energy bins, the number of inverted parameters is 36. The choice of the initial guess is crucial for the minimization
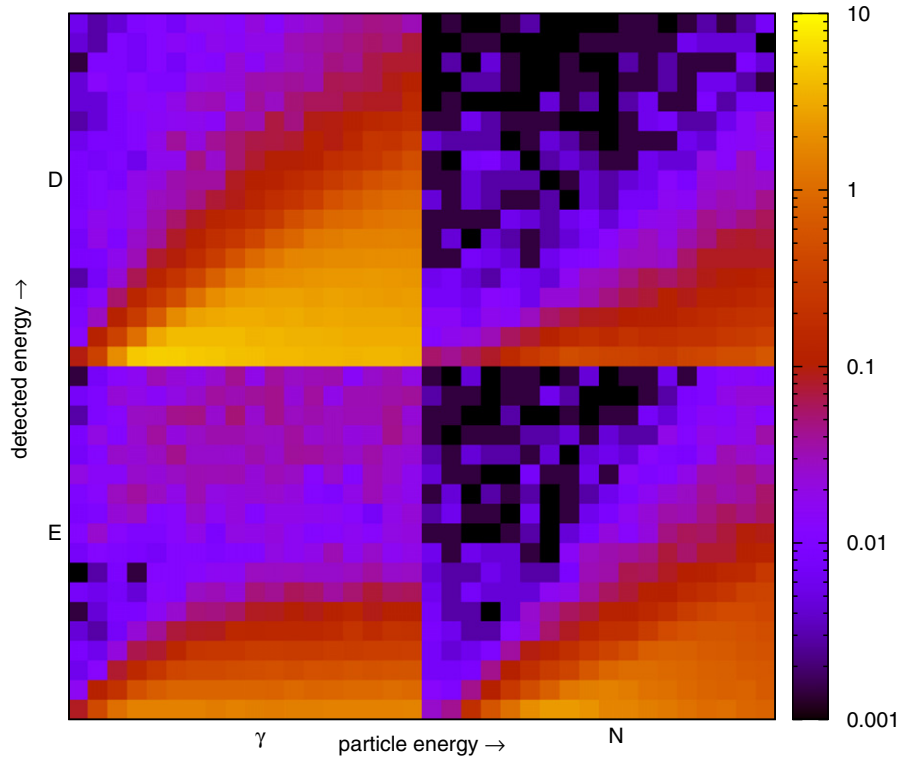
Fig. 2. Geometric factor matrices calculated with `GEANT4`. The color denotes the geometric factor [cm^2 sr] times the probability of detecting a gamma/neutron with an energy E in a certain measurement channel. The matrix consists of the four submatrices $\mathbf{A}_{D,\gamma}$, $\mathbf{A}_{D,N}$, $\mathbf{A}_{E,\gamma}$ and $\mathbf{A}_{E,N}$. For each submatrix the detector response is shown in 18×18 bins where the x-axis is primary particle energy [1–19 MeV] and the y-axis is the detector response [measurement channels 2500–7000].

algorithm to find a minimum which is close to the global minimum. Although the minimization requires no knowledge of the functional behavior of the input spectrum, an initial guess which is close to the solution significantly improves the result.

Instead of searching the parameter space for initial guesses from a purely mathematical perspective, we chose to provide initial guesses from a more physical point of view.

We begin with a first initial guess which would provide the correct solution for a detector with a response matrix which merely consists of diagonal elements

$$f_{i,\text{init}} = \frac{z_i}{\sum_j a_{ji}}. \tag{10}$$

Although the solution for this initial guess differs significantly from $\vec{f}$ in most cases, it gives a first impression of the intensity of gamma I_γ and neutron I_N spectra.

Since computation time is becoming increasingly cheaper, it is no problem to invert the measurement for a large number of differing initial guesses, e.g., different monoenergetic neutron beams. For poor initial guesses, one of the problems encountered is that the inverted solution often exhibits unphysical features, for instance, alternating high and low counts per bin. To address this, we scale the next initial guess with the integral inverted spectrum, and repeat the inversion procedure. Most of the times it takes ≈ 4 inversions to find the optimal intensity for an initial guess. We repeat this procedure with varying estimates of the neutron beam energy. For each such full inversion, we evaluate the merit function, and subsequently choose the best inversion. This results in our best estimate for the energy and intensity of the incident calibration neutron beam. Not unexpectedly, we obtained the correct values of ~ 15 and 19 MeV.

We found that slightly improved solutions could be found by randomizing the best inversion and using it as a new initial guess. The randomization was achieved by

$$f_{i,\text{init}} = f_i(1 + a\xi), \tag{11}$$

where $0 < a < 1$ and ξ is a uniformly distributed random variable in the interval $[-1, 1]$.

To test the stability of this algorithm for multiple beams or other functional behaviors, we mixed the measured data of the two beams taking 25% of the 14.8 MeV and 100% of the 19 MeV calibration measurements. With this new set of 'measurements' we repeated the procedure described above, but allowed for/selected multiple optimal solutions (in the sense of optimal merit functions). We then inverted all combinations of these optimal solutions to find the optimal combination. This could be a combination of many incident neutron beam energies. Nevertheless, in this fashion, we obtained neutron beams of ~ 15 and 19 MeV in proportion similar to their admixture. This same procedure was also applied to the single-energy neutron beams (15 and 19 MeV) separately. In that case no combination could improve the single-energy result.

Thus, the algorithm presented here is capable of reliably inverting measurements from multiple beams without any explicit or implicit knowledge of the number of beams or their respective energies.

4.3. Comparing inversion methods

In this subsection we compare the inversion results using the algorithm described above, but with three different merit functions, Poissonian, non-negative least-squares, and straight-forward chi-squared. To compare various inversion methods, an accurate knowledge of the error bars is required. We computed them with
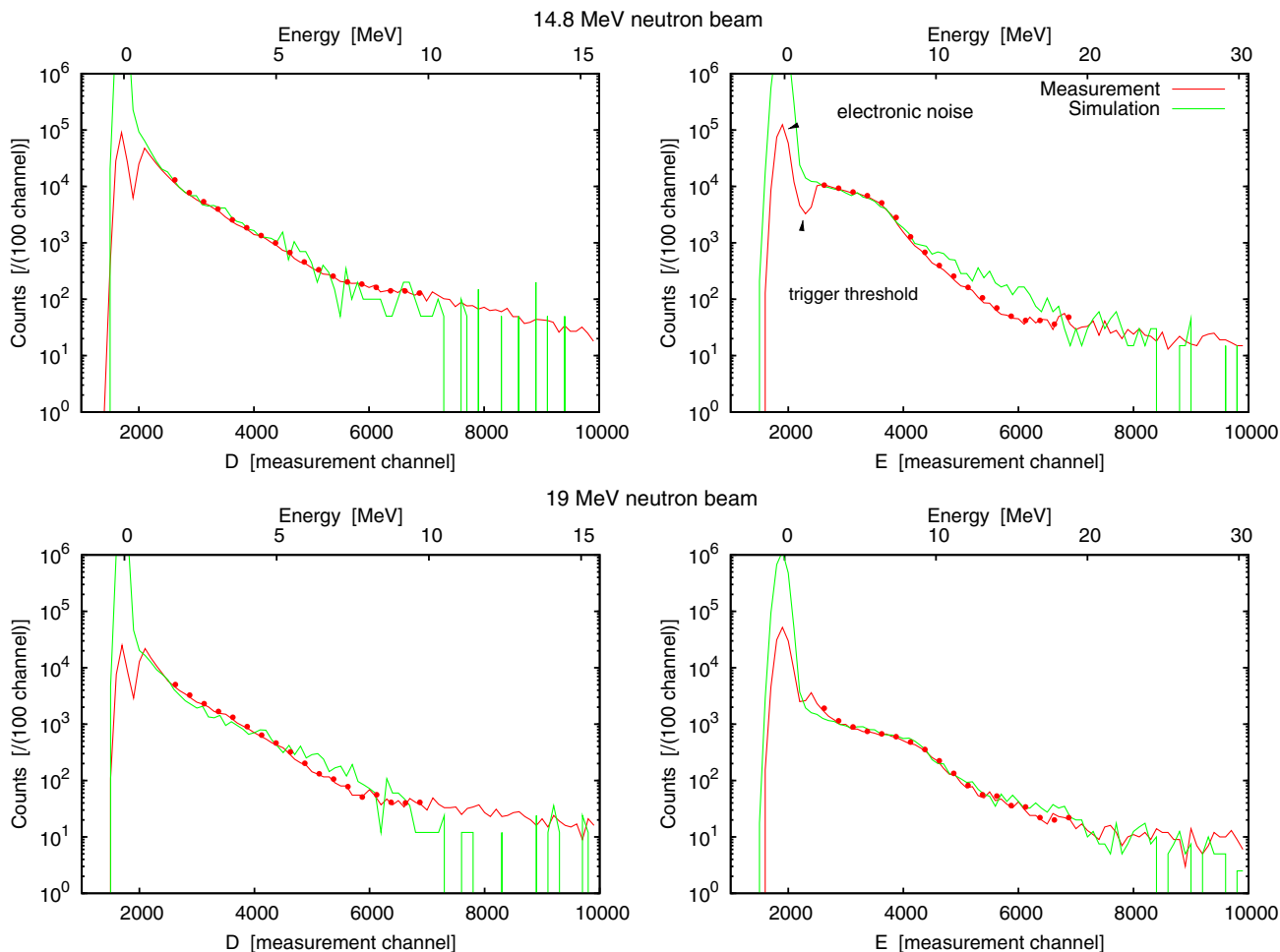
Fig. 3. PTB calibration measurement (red) and simulation (green) for the 14.8 MeV (top) and 19 MeV (bottom) neutron beam for the **D** (left) and **E** detector (right). Measurements are compared with a 10^6 particle GEANT4 simulation. Measurements and simulations match very well for both detectors. Because the trigger threshold is not included in the simulation we do not expect agreement in measurement channels $\leqslant 2500$. The red dots show the corresponding measurement vectors $\vec{z}_D$, $\vec{z}_E$ which are binned to match the detector response matrix from Fig. 2. To allow better comparison their intensities are reduced by a factor of 4, corresponding to the increased bin size.

a bootstrap Monte-Carlo method of the neutron-beam measurements similar to that described, e.g., in [21]. Based on the actual data set, a number of synthetic data sets are generated. In each synthetic dataset a random fraction of the original points are replaced by duplicated original points, for each synthetic dataset a measurement histogram $\vec{z}$ is calculated and inverted.

Fig. 4 shows the resulting inversions for the 14.8 MeV neutron beam and the 19 MeV neutron beam in the top two panels. As described above, an additional combined measurement vector from the 14.8 and 19 MeV measurement $\vec{z} = 0.25\vec{z}_{14.8\text{MeV}} + \vec{z}_{19\text{MeV}}$ was inverted, the results are shown in the lower panel. For all methods the neutron beams can be identified remarkably well. However a gamma background is also found. Unfortunately, the spectrum of the induced gamma radiation is not known, therefore we have no way of determining the accuracy of the inverted gamma spectrum.

For the 14.8 MeV neutron beam both the chi-square and the Poisson method show a clear beam in the 14.5 MeV energy bin, the NNLS inversion finds most neutrons in the 15.5 MeV bin and only few neutrons in the 14.5 MeV bin. The chi-square method finds some neutrons in the 12.5 MeV bin. For the 19 MeV neutron beam all methods clearly identify the 19 MeV neutrons and do not show any significant deviation in intensities. Although not as clear as for the 14.8 and 19 MeV measurement, the combined neutron beams are clearly resolved. As before the NNLS method finds the maximum of the 14.8 MeV beam in the 14.5 MeV bin. In contrast

to the 14.8 MeV measurement, the chi-square method finds no neutrons at 12.5 MeV. The inverted beam intensities differ from method to method. This is especially visible for the 19 MeV beam of the combined measurement. While the Poisson and chi-squared methods reproduce the total number of counts in the two separate neutron beams, the NNLS method overestimates the 19 MeV intensity.

The results shown in Fig. 4 were obtained using the randomization of initial guesses described above. This improved the Poisson merit function considerably, but had a much lesser effect on the NNLS and chi-squared merit functions. Our interpretation is that NNLS and chi-square perform much better in finding the global minimum.

5. Monte-Carlo measurements in a simulated Martian radiation environment

The demonstrated inversion methods performed very well for a beam of monoenergetic neutrons and a combination thereof. Those input spectra are however, quite different from the expected neutron and gamma spectra on Mars. In the previous section we showed that the detector response matrix describes the detector behavior correctly for 14.8 and 19 MeV neutrons. In this section we assume the detector response matrix as correct and use it to generate Monte-Carlo detector measurements. The expected
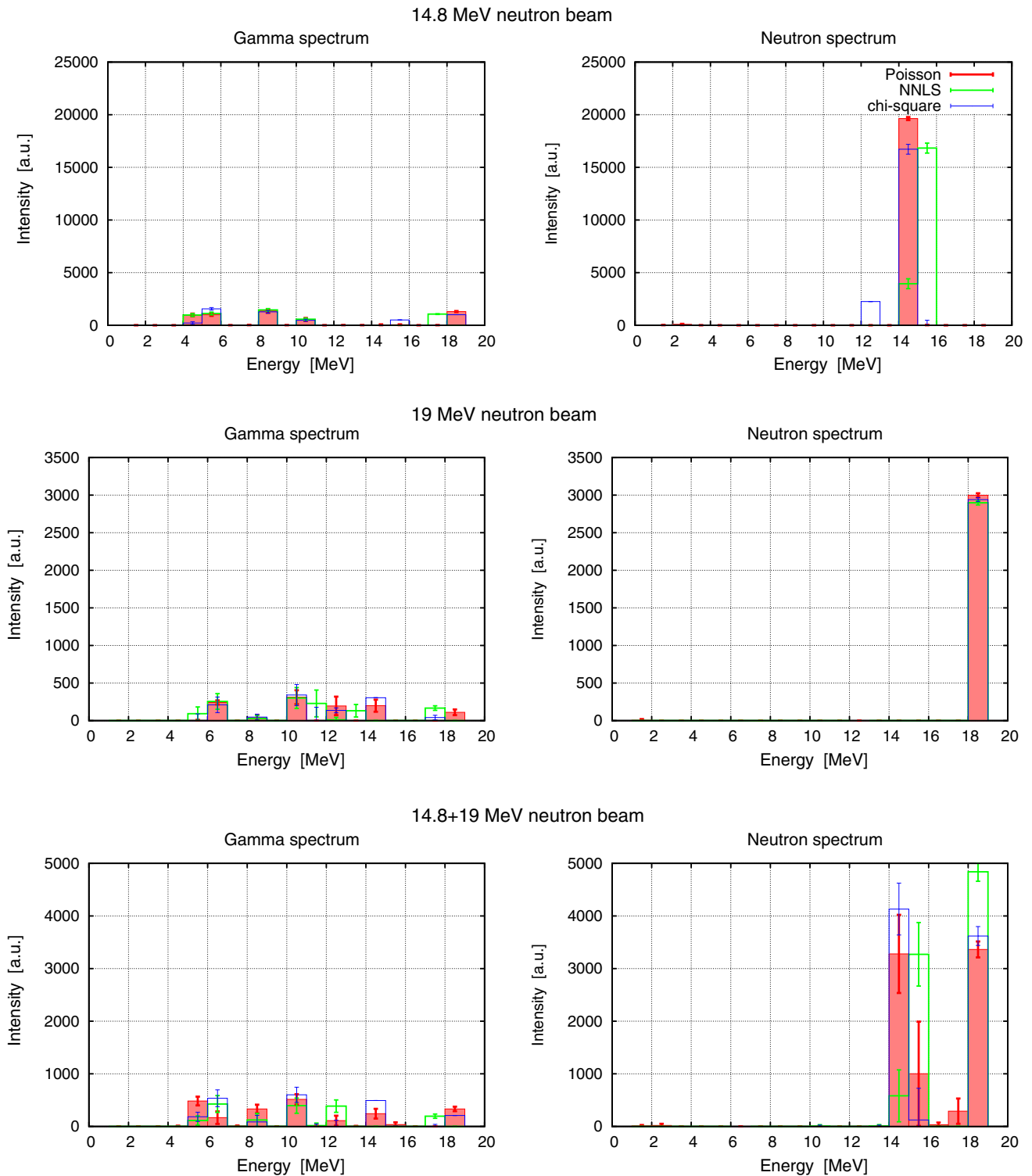
Fig. 4. Inverted PTB calibration measurements for the 14.8 and 19 MeV beam and a combined measurement of both beams $\vec{z} = 0.25\vec{z}_{14.8\text{MeV}} + \vec{z}_{19\text{MeV}}$. All methods can clearly identify the neutron beam at the correct position. For the combined measurement, the 14.8 MeV beam is distributed into two energy bins, but for the Poisson and chi-square inversion the intensities of the beam are the same as in the single measurements.

GCR-proton and helium induced, omnidirectional neutron and gamma flux on the Martian surface $\vec{f}$ are calculated with PLANETO-COSMICS [22] for present day Mars at ground level under solar minimum conditions.

To generate an artificial measurement $\vec{z}$, each column of the response matrix is used as a probability distribution function. For each energy bin a number of particles, given by the input spectrum,

is distributed according to this probability distribution. This way a large number of Monte-Carlo measurements can be generated to evaluate the performance of different inversion methods dependent on available statistics, i.e., the number of detected particles.

The artificial measurements generated as just discussed were then inverted with the methods described above. As initial guesses, we used various power laws and also some functional shapes

which were based on the expected spectra but different from these.

The black curve in the top (bottom) panel of Fig. 5 shows the average of 1000 generated gamma (neutron) spectra. Together, they consist of a total of 200,000 particles. These artificial spectra were inverted, the mean results $\langle f_i \rangle$ are shown as solid dots together with the corresponding mean errors $\langle \Delta f_i \rangle$ for each energy bin. As for the calibration neutron beam inversion, the errors for each inversion, Δf_i, were computed via bootstrap Monte Carlo. The mean is always within a factor of two of the average input spectrum. However, this good agreement of the average inversion does not guarantee that individual spectra also agree well with the input spectra. The errors however, give information about the uncertainty of each inverted spectrum and are plotted as an error bar in the same color as the mean. The mean and the errors for the Poisson and chi-squared methods are slightly shifted by ±0.1 MeV to enhance readability. The errors are small compared to the mean of the inverted spectra only for the low energy bins where count rates are high. All methods perform well for gammas, but the Poisson method produces significantly better results for neutrons where NNLS and chi-square method show large errors for energies above 4 MeV.

To compare the accuracy of the three studied inversion methods, we have plotted the relative erros $\langle \Delta f(E) \rangle / \langle f(E) \rangle$ of the inverted
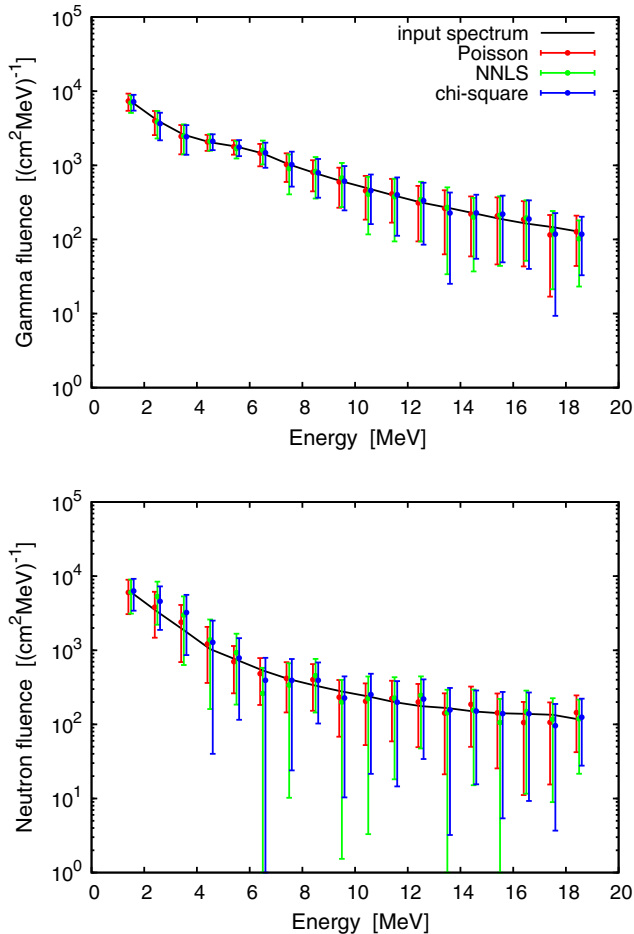
spectra in Fig. 6 for 200,000, 500,000 and 1,000,000 generated particle events using the same color code as in Fig. 5. While the NNLS and the chi-square methods produce similar results, the Poisson method produces clearly better results for neutron and slightly better results for gammas. As expected, the relative errors decrease with an increasing number of generated particles. Interestingly, the
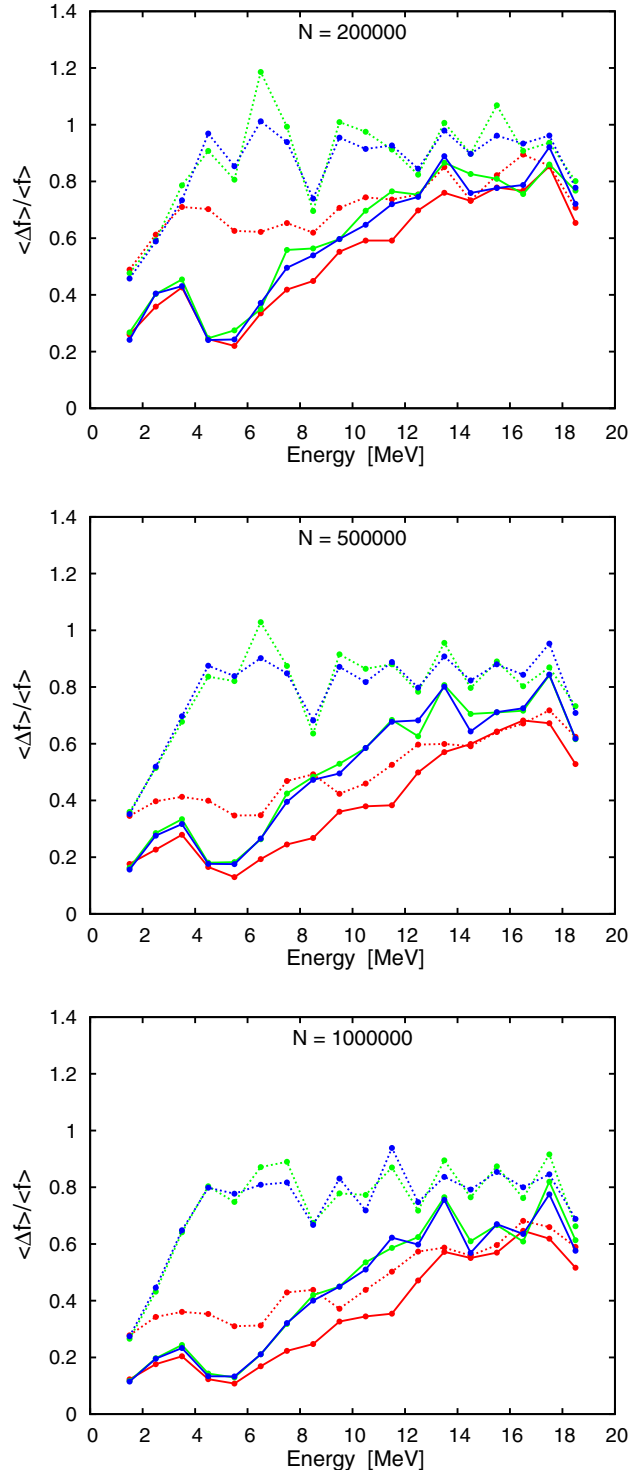

Fig. 5. Average gamma (top) and neutron (bottom) spectra for 1000 Monte-Carlo generated measurements of as expected on the Martin surface are shown as a blackline. A total of 200,000 particles were generated, which corresponds to ~3400 s (i.e., about an hour) of exposure for RAD. The mean $\langle f_i \rangle$ values and the mean errors $\langle \Delta f_i \rangle$ of the inverted spectra are shown for the Poisson, NNLS and chi-square methods in red, green, and blue, respectively. To enhance visibility, data points for the chi-square and the Poisson method have been shifted by ± 0.1 MeV.

Fig. 6. Relative error $\langle \Delta f(E) \rangle / \langle f(E) \rangle$ for 200,000, 500,000 and 1,000,000 generated particles, for the Poisson (red), NNLS (green) and chi-square (blue) methods. Relative errors of the inverted gamma spectra are plotted as solid lines and as dashed lines for neutrons.

J. Köhler et al. / Nuclear Instruments and Methods in Physics Research B 269 (2011) 2641–2648

Poisson method shows a large improvement for neutrons, while NNLS and chi-square method show only moderate improvements.

As in the previous section the NNLS and chi-square method could not be improved using randomized initial guesses. As in Section 4 the results of the Poisson method could be improved in this more realistic case as well.

6. Discussion and conclusion

We compared three inversion techniques for gamma-neutron measurements with the MSL RAD instrument. Instead of fitting a known functional behavior to the measured data, the inversion treats each energy bin of the inverted spectrum as a free parameter. All analyzed methods use a merit function, which is minimized, to find the input spectra for a measurement. All methods reconstruct the known input spectrum for the neutron beam calibration measurement performed at the PTB.

We investigated the effect of increased counting statistics for all three methods using Monte-Carlo generated "measurements" of the expected Martian input spectra.

To give a quantitative overview of the performance of the different methods the mean relative errors and their runtime are shown in Tables 1 and 2. As already apparent in Fig. 6, the Poisson method clearly produces more accurate results than the NNLS and chi-square method. The uncertainties of the Poisson method are between 10% and 30% smaller than for the NNLS and chi-square method. Nevertheless, one should note that the results from the Poisson method are strongly improved using an additional randomization of the initial guesses, while the other methods do not improve significantly and seem to be better at finding the global minimum even for inaccurate initial guesses. This increases the number of necessary initial guesses for the Poisson method, however, even including this extra burden, the Poison method is still faster than the two other methods by a factor of ~1.5. For both the PTB neutron measurement and the artificial Martian measurements, the Poisson method performed as good as-or better than the NNLS or chi-square method. Comparing performance and runtime for the different methods, the Poisson method is the most promising candidate for the future inversion of Martian gamma/neutron measurements with RAD.

In general, the instrument response function, **A**, is singular and, therefore, not invertible. In our case, it turns out that **A** is non-singular and invertible. Therefore, any measurement can, in principle, be inverted $\vec{z} = \mathbf{A} \cdot \vec{f} \Longleftrightarrow \vec{f} = \mathbf{A}^{-1} \cdot \vec{z}$, however, for measurements plagued by stochastic noise, such as a counting process with finite countrates this approach rarely produces accurate and useful results. Application of this "method" to the inversion of the PTB neutron beams resulted in large alternating positive and negative values with no resemblance at all to the neutron beam. For Monte-Carlo measurements this method started to produce results with similar quality as the minimizations for $N \gg 10^7$ particles, i.e., requiring at least 10–50 times better counting statistics than the inversion methods described above in this paper.

The demonstrated measurement and inversion of the Martian neutron/gamma spectra should not be viewed as a final estimation of the instruments performance, but as a proof of concept. The resulting spectra can be improved tremendously when fitting less energy bins or an expected functional behavior, such as a power law.

One remaining problem is the discontinuity in the GEANT4 neutron interaction process, which at the moment restricts the response matrix to energies below 19 MeV. Neutron beam measurements for energies above 20 MeV are planned and will allow us to extend the detector response matrix.

References

[1] S. Brandt, Data Analysis: Statistical and Computational Methods for Scientists and Engineers, Springer-Verlag, Newyork, 1999.
[2] M. Bertero, P. Boccacci, Introduction to Inverse Problems in Imaging, IOP Publishing, Ltd., Bristol, 1998.
[3] C.R. Vogel, Computational Methods for Inverse Problems, SIAM, Philadelphia, 2002.
[4] J.P. Kaipio, E. Somersalo, Computational and Statistical Methods for Inverse Problems, Springer, Berlin, 2005.
[5] C.L. Lawson, R.J. Hanson, Solving Least Squares Problems (Classics in Applied Mathematics 15), Society for Industrial Mathematics, 1987.
[6] A. Björck, Numerical Methods Foar Least Squares Problems, SIAM, Philadelphia, 1996.
[7] E.A. Böhm, A. Kharytonov, R.F. Wimmer-Schweingruber, Solar energetic particle spectra from the SOHO-EPHIN sensor by application of regularization methods, A&A 473 (2) (2007) 673–682.
[8] J. Sheng, L. Ying, A fast image reconstruction algorithm based on penalized-likelihood estimate, Medical Engineering & Physics 27 (2005) 679–686.
[9] J.M. Bardsley, Stopping rules for a nonnegatively constrained iterative method for ill-posed Poisson imaging problems, BIT Numerical Mathematics 48 (2008) 651–664.
[10] E.D. Nowak, E.D. Kolaczyk, A statistical multiscale framework for Poisson inverse problems, IEEE Transactions on Information Theory 46 (5) (2000) 1811–1825.
[11] K.E. Batkov, A.D. Panov, J.H. Adams, et al., Deconvolution of energy spectra in the ATIC experiment, in: Proceedings of the 29th International Cosmic Ray Conference, Pune, India, August 3–10, 2005, vol. 3, 2005, pp. 353–356.
[12] T. Hauschild, M. Jentschel, Comparison of maximum likelihood estimation and chi-square statistics applied to counting experiments, Nuclear Instruments and Methods in Physics Research, Section A 457 (2001) 384–401.
[13] M.D. Hannam, W.J. Thompson, Estimating small signals by using maximum likelihood and Poisson statistics, Nuclear Instruments and Methods in Physics Research, Section A 431 (1999) 239–251.
[14] W.T. Eadie, Statistical Methods in Experimental Physics, Elsevier Science Ltd., 1983.
[15] E. Jones, T. Oliphant, P. Peterson, et al., 2001, SciPy: Open source scientific tools for Python. Available from: <http://www.scipy.org/>.
[16] S. Zhu, R.H. Byrd, L. Lu, J. Nocedal, Algorithm 778: L-BFGS-B: Fortran subroutines for large-scale bound-constrained optimization, ACM Transactions on Mathematical Software 23 (4) (1997) 550–560.
[17] R.H. Byrd, P. Lu, J. Nocedal, C. Zhu, A Limited-Memory Algorithm for Bound Constrained Optimization, 1994.
[18] S. Agostinelli et al., GEANT4A simulation toolkit, Nuclear Instruments and Methods in Physics Research Section A: Accelerators, Spectrometers, Detectors and Associated Equipment 506 (3) (2003) 250–303.
[19] O. Kortmann, Scintillator Performance Investigation for MSL/RAD, Ph.D. Thesis, 2010.
[20] R. Nolte, M.S. Allie, R. Böttger, F.D. Brooks, A. Buffler, V. Dangendorf, H. Friedrich, et al., Quasi-monoenergetic neutron reference fields in the energy range from thermal to 200 MeV, Radiation Protection Dosimetry 110 (2004) 37–102.
[21] W.H. Press, Numerical Recipes: The Art of Scientific Computing, Cambridge University Press, 2007.
[22] L. Desorgher, E.O. Flückiger, M. Gurtner, 2006. The PLANETOCOSMICS Geant4 application 36th COSPAR Scientific Assembly, 36, 2361.

Table 2
The runtime, given in units of runtime for the Poisson method, for 200,000, 500,000 and 1,000,000 generated particles.

N	Poisson	NNLS	Chi-square
200,000	1	1.47	1.24
500,000	1	1.56	1.30
1,000,000	1	2.40	1.81

Table 1
The mean relative errors for 200,000, 500,000 and 1,000,000 generated particles.

N	Poisson	NNLS	Chi-square
200,000	0.65	0.74	0.72
500,000	0.45	0.65	0.65
1,000,000	0.41	0.59	0.59